

Headgroup dimerization in methanethiol monolayers on the Au(111) surface: a density functional theory study

Jian-Ge Zhou, Quinton L. Williams, Frank Hagelberg
*Computational Center for Molecular Structure and Interactions,
 Department of Physics, Atmospheric Sciences, and Geoscience,
 Jackson State University, Jackson, MS 39217, USA*

A long-standing controversy related to the dimer pattern formed by S atoms in methanethiol (CH_3SH) on the Au(111) surface has been resolved using density functional theory. For the first time, dimerization of methanethiol adsorbates on the Au(111) surface is established by computational modeling. For methylthiolate (CH_3S), it is shown that the S atoms do not dimerize at high coverage but reveal a dimer pattern at intermediate coverage. Molecular dynamics simulation at high coverage demonstrates that the observed dialkyl disulfide species are formed during the desorption process, and thus are not attached to the surface.

PACS numbers: 61.46.-w, 36.40.Cg, 68.43.Bc

I. INTRODUCTION

Recently, much attention has focused on the properties of self-assembled monolayers (SAM), particularly of alkanethiol on gold surfaces [1]–[14]; see Ref. [15] for a review. This high level of interest may be ascribed to their relevance to wetting phenomena, tribology, chemical and biological sensing, optics and nanotechnology. Despite the apparent simplicity of these systems, their observation in various experiments has led to contradictory results, in particular related to the question if the S-H headgroups of alkanethiol organize in dimers on the Au(111) surface or not.

In the early phase of SAM related studies, it was assumed that alkanethiol adsorbs at threefold coordinated hollow sites on the Au(111) surface [15]. This picture has been first challenged by grazing incidence X-ray diffraction (GIXRD) studies [1, 2], where a dimer pattern was proposed. High-resolution electron-energy-loss spectra supported this dimer model [3]. Scanned-energy and scanned-angle photoelectron diffraction experiments on alkanethiolate, in contrast, did not yield any dimerization [8, 9]. Based on temperature-programmed desorption, Auger electron spectroscopy, and scanning tunneling microscopy (STM) studies, methanethiol was found to form dimers [10]. Recently, Torrelles et al. observed by use of GIXRD, STM and electrochemical techniques that alkanethiolate does not dimerize [13].

The present contribution addresses these controversial observations by simulation from first principles. A consistent model is proposed that agrees with all available experimental data related to thiol adsorption on the Au(111) surface. Until recently, it was assumed that the S-H bond of methanethiol is cleaved once it is adsorbed to the Au(111) surface, such that it becomes methylthiolate [4, 15]. Thus, methanethiol and methylthiolate would exhibit the same adsorption pattern once deposited on Au(111). Recent results, however, show that methanethiol stays intact when in contact with the defect-free Au(111) surface [11, 12], and

turns into methylthiolate on Au(111) only in the presence of vacancies. To examine if methanethiol dimerizes on Au(111), it is crucial to study the methanethiol and methylthiolate dimer patterns separately. If these two species display different adsorption structures, the long-standing controversy related to their dimerization behavior might be resolved.

Guided by this motivation, we study in the present contribution the adsorption of methanethiol and methylthiolate on the Au(111) surface by use of density functional theory [16]. First, we will present adsorption energies and geometries for methanethiol on the regular Au(111) at 0.5 ML and 1.0 ML, and demonstrate, for the first time, that methanethiol reorganization on the clean Au(111) surface gives rise to the formation of a dimer pattern. Subsequently, we will show that methylthiolate on the regular Au(111) surface exhibits a coverage dependent dimerization behavior. Further, we address the possible impact of surface defects and perform molecular dynamics (MD) simulations to inspect the effect of temperature on the dimer formation.

II. COMPUTATIONAL METHOD

We employ the VASP code [16] which involves the projector augmented wave potential [17, 18] and the PW91 generalized gradient approximation [19]. The wave functions are expanded in a plane wave basis with an energy cutoff of 400 eV. The Brillouin zone integration is performed by use of the Monkhorst-Pack scheme [20]. We utilized a $3 \times 3 \times 1$ k point mesh for the geometry optimization. A $(3 \times 2\sqrt{3})$ superlattice (see Fig. 1a) is employed as an Au(111) supercell [5], corresponding to 12 Au atoms per layer. The Au atoms in the top three atomic layers are allowed to relax, while those in the bottom layer are fixed to simulate bulk-like termination [21]. The vacuum region comprises seven atomic layers, which exceeds substantially the extension of the methanethiol molecule. To examine the accuracy of our approach we

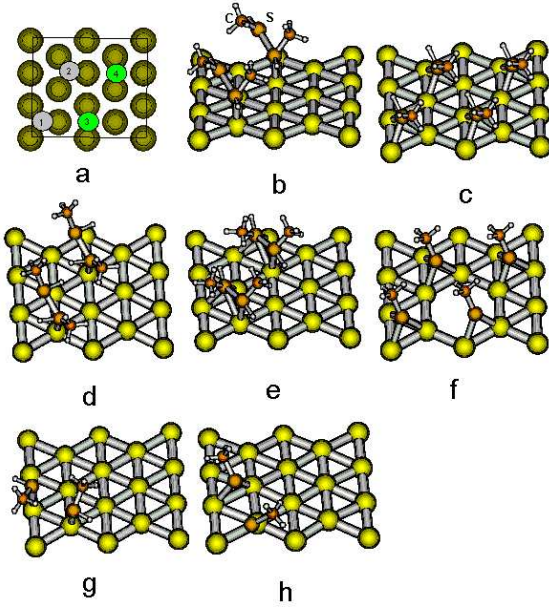


FIG. 1: (Color online) (a) $(3 \times 2\sqrt{3})$ supercell. (b) top+hcp. (c) hcp-hcp. (d) top+hcp'. (e) top+fcc+3b. (f) hcp-hcp* with a vacancy. (g) top+top. (h) top+fcc+3b'.

increased the energy cutoff to 500 eV and the number of k points to $8 \times 8 \times 1$. In both cases, the difference amounted to less than 2%. We further calculated the gold lattice constant, and found it to agree with the experimental value [22] within 2.1%.

III. RESULTS AND DISCUSSION

A. Methanethiol molecules deposited on the regular Au(111) surface

In what follows we present our results, beginning with a discussion of both the geometries and adsorption energies for the optimized configurations of methanethiol on the regular Au(111) surface at 0.5 ML (Fig. 1g, Fig. 1h) and 1.0 ML (Fig. 1b - Fig. 1f) coverage, as displayed in Table I. At 1.0 ML, we arrange four methanethiol molecules in the $(3 \times 2\sqrt{3})$ supercell according to the experimentally detected structure [23, 24]. The molecules labeled 1(3) and 2(4) are symmetry equivalent, see Fig. 1a. The nomenclature top+hcp in Table I refers to an initial geometry where the S atom of adsorbate 1 is placed on an exact top site, while that of adsorbate 3 is just in an fcc region so that the distance between the S atoms of 1 and 3 is close to 2.3 \AA (see Fig. 1b), and analogously for the notations bri+hcp, hcp+fcc, etc. In Fig. 1, the S and C atoms are distinguished by ball symbols of different sizes. The symbol hcp-hcp in Table I indicates that the S atoms of both, adsorbates 1 and 3, are placed exactly at a hcp center too (Fig. 1c), with analogous definitions for the symbols bri-bri, top-top etc. The

TABLE I: The geometries and adsorption energies for the studied methanethiol configurations on the regular Au(111) surface at 0.5 ML and 1.0 ML. The entries d_{S-S} , d_{S-Au} (in \AA) and E_{ads} (in eV/per methanethiol) refer to the S-S bond length, the shortest Au-S bond length and the adsorption energy, respectively. The superscripts *I* and *E* stand for the initial and equilibrium structures, respectively. The maximum adsorption energy is underlined.

| Initial | d_{S-S}^I | 0.5ML | | | 1.0ML | | |
|-------------|-------------|-------------|--------------|-------------|-------------|--------------|-------------|
| | | d_{S-S}^E | d_{S-Au}^E | E_{ads} | d_{S-S}^E | d_{S-Au}^E | E_{ads} |
| bri+fcc | 2.30 | 3.36 | 2.69 | 0.46 | 3.76 | 3.02 | 0.23 |
| bri+fcc' | 2.30 | 3.69 | 3.05 | 0.37 | 3.74 | 2.99 | 0.23 |
| bri+hcp | 2.30 | 3.51 | 2.86 | 0.42 | 4.23 | 2.83 | 0.25 |
| bri+hcp' | 2.30 | 3.78 | 2.93 | 0.38 | 3.74 | 2.98 | 0.23 |
| bri-bri | 3.90 | 4.20 | 2.93 | 0.24 | 4.01 | 2.73 | 0.18 |
| bri-top | 3.90 | 3.65 | 2.89 | 0.31 | 3.66 | 3.21 | 0.15 |
| fcc+hcp | 2.30 | 4.47 | 2.79 | 0.46 | 3.07 | 2.63 | 0.19 |
| fcc+hcp' | 2.30 | 3.73 | 2.71 | 0.40 | 3.73 | 2.45 | -1.99# |
| fcc-bri | 3.70 | 4.35 | 2.88 | 0.28 | 3.95 | 3.03 | 0.18 |
| fcc-fcc | 5.00 | 5.08 | 3.15 | 0.24 | 5.08 | 3.67 | 0.15 |
| fcc-top | 3.40 | 3.88 | 3.17 | 0.29 | 3.83 | 3.21 | 0.14 |
| hcp+fcc | 2.30 | 4.28 | 2.77 | 0.44 | 3.10 | 2.69 | 0.21 |
| hcp+fcc' | 2.30 | 3.62 | 2.73 | 0.40 | 3.06 | 2.47 | -0.70# |
| hcp-bri | 4.20 | 4.23 | 3.17 | 0.24 | 4.24 | 3.12 | 0.18 |
| hcp-fcc | 3.40 | 4.11 | 3.11 | 0.23 | 4.00 | 3.29 | 0.18 |
| hcp-hcp | 5.00 | 5.08 | 3.16 | 0.23 | 5.08 | 3.60 | 0.14 |
| hcp-hcp* | 5.00 | 5.08 | 3.08 | 0.25 | 5.08 | 3.33 | 0.15 |
| hcp-top | 4.50 | 4.96 | 3.05 | 0.29 | 4.26 | 3.47 | 0.21 |
| top+fcc | 2.30 | 3.50 | 2.65 | 0.40 | 3.15 | 2.57 | 0.20 |
| top+fcc+3b | 2.30 | 3.43 | 2.68 | 0.46 | 3.25 | 2.80 | 0.20 |
| top+fcc' | 2.30 | 3.21 | 2.68 | 0.37 | 3.74 | 3.26 | -0.59# |
| top+fcc+3b' | 2.30 | 3.21 | 2.76 | 0.31 | 3.61 | 2.48 | -2.03# |
| top+hcp | 2.30 | 3.48 | 2.68 | 0.39 | 3.54 | 2.64 | <u>0.26</u> |
| top+hcp+3b | 2.30 | 3.48 | 2.65 | 0.43 | 3.85 | 3.14 | 0.25 |
| top+hcp' | 2.30 | 3.26 | 2.67 | 0.39 | 3.27 | 2.82 | 0.25 |
| top+hcp+3b' | 2.30 | 3.27 | 2.79 | 0.32 | 3.29 | 2.85 | 0.21 |
| top+top | 2.30 | 3.58 | 2.70 | <u>0.48</u> | 3.36 | 2.88 | 0.23 |
| top-top | 5.00 | 5.08 | 3.03 | 0.36 | 5.08 | 3.17 | 0.19 |
| top-top' | 5.90 | 5.96 | 3.04 | 0.35 | 3.67 | 2.77 | 0.20 |

arrangements top+hcp' (Fig. 1d) and top+hcp differ by the dihedral angle of the two S-C bonds, and accordingly for other primed structures. The top+fcc+3b configuration is shown in Fig. 1e, where the S-S group forms three bonds with the surface.

From Table I, at 0.5 ML the adsorption energy for the most stable structure is 0.48 eV (top+top, see Fig. 1g), and the S adsorption sites are on the top of Au atoms, in keeping with recent experimental results [10]. The S-S distance is about 3.6 \AA . Thus at 0.5 ML coverage a dimer is formed when methanethiol is adsorbed to the regular

Au(111) surface at low temperature. This dimerization was indeed observed recently by STM experiment at 5 K [10]. In Tables I, II and III, some configurations at 1.0 ML coverage are marked by #. These structures are not favored since they involve broken S-C bonds. From Table I, the adsorption energy of the stable configuration at 1.0 ML, with top+hcp as initial structure, is 0.26 eV. The optimized structure involves one S atom in the fcc region but tending toward the atop site; the other S atom locates in the fcc region, leaning toward the bridge site, in agreement with experimental findings [11]. The resulting S-S distance is about 3.6 Å. This implies methanethiol dimer formation also at 1.0 ML coverage.

The bond between the methanethiol and Au(111) involves an ionic contribution due to electron transfer proceeding from the surface to the adsorbate. This interaction is well described by the density functional theory (DFT) [25]. Our calculations yield an effective charge of -0.2 e, per methanethiol molecule. The binding energy of two pure methanethiol molecules, maintaining their spatial relation as realized on the surface, results as 0.03 eV by DFT [16], 0.02 eV using a coupled cluster with single, double and triple excitations (CCSD(T)/6-311+G(d,p)) [27], and the Van der Waals interaction between them is 0.06 eV [27]. Being higher than the CCSD(T) value by 50%, the DFT prediction for the interaction between two pure molecules is inaccurate, which is consistent with recent observations [28, 29]. However, the interaction that leads to dimerization is a surface mediated effect, which strongly exceeds the Van der Waals attraction between the dimer constituents [26]. To evaluate the surface mediated interaction between two dimer constituents, we study the case of 0.5 ML where the preferred configuration is the optimized top+top structure (Fig. 1g). Specifically, we consider the difference $\Delta E = E_{ad}^{(top+top)}(d_{S-S} = 3.58) - E_{ad}^{(top-top)}(d_{S-S} = 5.08)$, which is interpreted as a reorganization energy, namely the energy gain due to dimer formation by rearranging an initially even adsorbate distribution on the surface. This energy is 0.24 eV, and thus twelve times (0.24 eV/0.02 eV(CCSD(T))) larger than the weak interaction between two pure methanethiol molecules, maintaining their spatial relation as adopted on the surface. On the other hand, the interaction energy among two molecules and Au(111) is found to be 0.96 eV (top+top). The Van der Waals component is thus estimated to contribute only 6.3% (0.06 eV/0.96 eV) to the total interaction energy. Therefore, the methanethiol dimer formation is not caused by the Van der Waals force. Rather, it is a surface mediated effect. Since the energy difference between the dimer structures at a S - S distance of 3.6 Å [1, 2] and the reference situation of methanethiol adsorbates spread evenly over the Au(111) surface (d_{S-S} around 5.0 Å) [15] is minimally 0.24 eV at all coverage levels, for both methanethiol and methylthiolate, omission of the relatively small Van der Waals contribution does not change our conclusions regarding the dimerization effect.

B. Methylthiolate adsorbates on the regular Au(111) surface

Does methylthiolate exhibit the same dimerization behavior as methanethiol? Table II lists the configurations of methylthiolate on clean Au(111) at two levels of coverage, 0.5 ML and 1.0 ML, with the S-S distances close to 2.1 Å, 3.6 Å and 5.0 Å. The maximum adsorption energies for 0.5 ML and 1.0 ML, underlined in Table II, are 2.12 eV and 1.99 eV (per molecule). Table II shows that at 0.5 ML, the S-S distance is about 3.6 Å, which is indicative of a dimer (see Fig. 1h). At 1.0 ML, an S-S distance of 5.0 Å is found. In the light of this result, the absence of dimerization reported in [8] appears plausible. The respective measurement involved a coverage level of 1.0 ML, and from our simulation, no dimers emerge in this case. The lack of dimerization at 1.0 ML for methylthiolate as opposed to methanethiol is rationalized by the much stronger substrate-adsorbate interaction for the former than for the latter species, as shown by the entries for E_{ads} and d_{S-Au} in Tables I and II.

C. Methylthiolate adsorbates on the defected Au(111) surface

To examine if substrate defects induce S-S dimer formation, we allow for a vacancy in the top layer of the ($3 \times 2\sqrt{3}$) supercell [5] (see Fig. 1f). The location of this vacancy is chosen such that it affects as many methylthiolate adsorbates as possible. It is sufficient to include methylthiolate in this segment of our study since methanethiol reduces to methylthiolate when adsorbed to the defected Au(111) surface [11, 12]. Table III comprises the methylthiolate configurations in the presence of a vacancy at coverage levels of 0.5 and 1.0 ML.

With respect to dimer formation, the same observations are made as for the regular surface. The dimerization behavior of methylthiolate is therefore not impacted by the presence of defects.

D. Molecular Dynamical Simulation

In the following, we inspect the effect of temperature on methylthiolate dimerization. Two methylthiolate molecules are adsorbed on the top layer of one-half of the ($3 \times 2\sqrt{3}$) supercell, the resulting coverage being 1.0 ML. Fig. 2 shows the time variation of the S-S distance as resulting from MD simulation for a) methylthiolate on the regular Au(111) at 300K, b) at 400K, c) methylthiolate on the imperfect Au(111) surface at 400K, d) methanethiol on the regular Au(111) surface at 240K. At 300K, methylthiolate is still attached to the regular Au(111) surface, the S-S distance oscillates around 5.0 Å, which shows that the adsorbates do not dimerize at this temperature. As one raises the temperature to 400K,

TABLE II: The geometries and adsorption energies for methylthiolate adsorbed on the regular Au(111) surface at 0.5ML and 1.0ML coverage.

| Initial | d_{S-S}^I | 0.5ML | | | 1.0ML | | |
|-------------|-------------|-------------|--------------|-------------|-------------|--------------|-------------|
| | | d_{S-S}^E | d_{S-Au}^E | E_{ads} | d_{S-S}^E | d_{S-Au}^E | E_{ads} |
| bri+fcc | 2.30 | 2.07 | 2.70 | 2.01 | 2.05 | 3.07 | 1.82 |
| bri+fcc' | 2.30 | 3.43 | 2.49 | 1.84 | 3.16 | 2.41 | 1.68 |
| bri+hcp | 2.30 | 2.07 | 2.97 | 1.99 | 2.06 | 2.86 | 1.80 |
| bri+hcp' | 2.30 | 3.54 | 2.41 | 1.88 | 3.48 | 2.42 | 1.72 |
| bri-bri | 3.90 | 4.33 | 2.47 | 1.98 | 4.40 | 2.48 | 1.89 |
| bri-top | 3.90 | 4.09 | 2.38 | 1.92 | 4.14 | 2.39 | 1.86 |
| fcc+hcp | 2.30 | 2.07 | 2.61 | 2.00 | 2.06 | 2.71 | 1.87 |
| fcc+hcp' | 2.30 | 3.34 | 2.40 | 1.90 | 3.28 | 2.48 | 1.35# |
| fcc-bri | 3.70 | 4.31 | 2.43 | 1.92 | 4.37 | 2.42 | 1.81 |
| fcc-fcc | 5.00 | 5.08 | 2.45 | 2.08 | 5.08 | 2.48 | <u>1.99</u> |
| fcc-top | 3.40 | 4.15 | 2.39 | 1.91 | 4.89 | 2.46 | 1.97 |
| hcp+fcc | 2.30 | 2.07 | 2.58 | 1.98 | 2.06 | 2.69 | 1.86 |
| hcp+fcc' | 2.30 | 3.31 | 2.40 | 1.83 | 3.54 | 2.45 | 1.39# |
| hcp-bri | 4.20 | 3.88 | 2.44 | 1.91 | 3.83 | 2.44 | 1.91 |
| hcp-fcc | 3.40 | 3.83 | 2.45 | 1.90 | 3.85 | 2.44 | 1.78 |
| hcp-hcp | 5.00 | 5.08 | 2.47 | 2.04 | 5.08 | 2.49 | 1.96 |
| hcp-hcp' | 5.00 | 5.08 | 2.47 | 2.10 | 5.08 | 2.47 | <u>1.99</u> |
| hcp-top | 4.50 | 4.50 | 2.39 | 1.88 | 4.80 | 2.50 | 1.80 |
| top+fcc | 2.30 | 2.06 | 2.72 | 2.00 | 2.05 | 2.81 | 1.88 |
| top+fcc+3b | 2.30 | 2.07 | 2.78 | 2.00 | 2.07 | 2.92 | 1.87 |
| top+fcc' | 2.30 | 2.05 | 2.83 | 2.00 | 3.59 | 2.50 | 1.40# |
| top+fcc+3b' | 2.30 | 3.66 | 2.47 | <u>2.12</u> | 3.61 | 2.48 | -0.51# |
| top+hcp | 2.30 | 2.06 | 2.75 | 2.01 | 2.06 | 2.63 | 1.86 |
| top+hcp+3b | 2.30 | 2.07 | 2.80 | 2.00 | 2.05 | 3.08 | 1.80 |
| top+hcp' | 2.30 | 2.06 | 2.79 | 2.00 | 2.05 | 2.86 | 1.87 |
| top+hcp+3b' | 2.30 | 3.59 | 2.47 | 2.04 | 3.75 | 2.48 | 1.85 |
| top+top | 2.30 | 2.07 | 2.73 | 2.00 | 2.07 | 2.78 | 1.87 |
| top-top | 5.00 | 5.08 | 2.38 | 1.73 | 5.08 | 2.38 | 1.67 |
| top-top' | 5.90 | 5.84 | 2.38 | 1.71 | 2.12 | 2.65 | 1.84 |

however, the S-S distance reduces to 3.5 Å. The temperature increase weakens the molecule-surface bond and thus favors intermolecular bonding. This process leads to dimer formation. If the temperature is high enough and methylthiolate starts to desorb, two molecules join to form dimethyl disulfide (CH_3SSCH_3). Thus the observed dialkyl disulfide emerges during the desorption process, and does not exist on the surface [3, 11]. At 400K, methylthiolate forms a dimer on regular Au(111), while the S-S distance turns out to be 5.0 Å for imperfect Au(111), and no dimerization is found (Fig. 2(c)). In the presence of a vacancy, the interaction between methylthiolate and Au(111) is stronger than in the regular case [6, 12, 30], and interaction between the molecules is accordingly weaker. For methanethiol, no dimers exist at 240 K.

TABLE III: The geometries and adsorption energies for methylthiolate adsorbed on the Au(111) surface with a vacancy.

| Initial | d_{S-S}^I | 0.5ML | | | 1.0ML | | |
|-------------|-------------|-------------|--------------|-------------|-------------|--------------|-------------|
| | | d_{S-S}^E | d_{S-Au}^E | E_{ads} | d_{S-S}^E | d_{S-Au}^E | E_{ads} |
| bri+fcc | 2.30 | 2.07 | 2.55 | 2.00 | 2.06 | 2.75 | 1.85 |
| bri+fcc' | 2.30 | 3.25 | 2.44 | 2.43 | 3.30 | 2.42 | 2.04 |
| bri+hcp | 2.30 | 2.06 | 3.10 | 2.01 | 2.06 | 2.77 | 1.83 |
| bri+hcp' | 2.30 | 3.31 | 2.44 | 2.43 | 3.98 | 2.44 | 1.99 |
| bri-bri | 3.90 | 4.22 | 2.42 | 2.25 | 4.44 | 2.44 | 2.14 |
| bri-top | 3.90 | 4.53 | 2.37 | 2.13 | 4.25 | 2.38 | 2.13 |
| fcc+hcp | 2.30 | 2.06 | 2.53 | 2.01 | 2.06 | 2.70 | 1.87 |
| fcc+hcp' | 2.30 | 4.22 | 2.46 | 2.26 | 3.75 | 2.44 | 1.53# |
| fcc-bri | 3.70 | 5.00 | 2.42 | 2.32 | 4.19 | 2.46 | 1.99 |
| fcc-fcc | 5.00 | 5.23 | 2.37 | 2.04 | 4.92 | 2.39 | 1.99 |
| fcc-top | 3.40 | 4.56 | 2.37 | 2.12 | 4.75 | 2.44 | <u>2.20</u> |
| hcp+fcc | 2.30 | 2.07 | 2.54 | 2.08 | 2.07 | 2.55 | 1.95 |
| hcp+fcc' | 2.30 | 3.81 | 2.42 | 2.33 | 3.62 | 2.45 | 1.61# |
| hcp-bri | 4.20 | 4.55 | 2.42 | 2.37 | 3.87 | 2.42 | 2.12 |
| hcp-fcc | 3.40 | 4.51 | 2.43 | 2.40 | 3.78 | 2.41 | 2.14 |
| hcp-hcp | 5.00 | 5.16 | 2.36 | 1.98 | 4.97 | 2.44 | 2.17 |
| hcp-hcp' | 5.00 | 4.73 | 2.45 | 2.21 | 5.03 | 2.43 | 2.20 |
| hcp-top | 4.50 | 4.27 | 2.36 | 2.17 | 4.44 | 2.39 | 1.92 |
| top+fcc | 2.30 | 2.06 | 2.59 | 2.08 | 2.06 | 2.68 | 1.93 |
| top+fcc+3b | 2.30 | 2.07 | 2.60 | 2.01 | 2.07 | 2.71 | 1.95 |
| top+fcc' | 2.30 | 2.06 | 2.67 | 2.04 | 3.67 | 2.36 | 1.49# |
| top+fcc+3b' | 2.30 | 3.33 | 2.43 | <u>2.48</u> | 3.36 | 2.42 | 1.61# |
| top+hcp | 2.30 | 2.06 | 2.62 | 2.08 | 2.07 | 2.59 | 1.89 |
| top+hcp+3b | 2.30 | 2.07 | 2.59 | 2.02 | 2.08 | 2.57 | 1.89 |
| top+hcp' | 2.30 | 2.06 | 2.67 | 2.04 | 2.06 | 2.66 | 1.95 |
| top+hcp+3b' | 2.30 | 3.36 | 2.42 | 2.45 | 3.29 | 2.49 | 2.12 |
| top+top | 2.30 | 2.07 | 2.61 | 2.09 | 2.07 | 2.64 | 1.94 |
| top-top | 5.00 | 4.94 | 2.36 | 1.87 | 4.86 | 2.43 | 2.16 |
| top-top' | 5.90 | 5.85 | 2.37 | 1.86 | 2.14 | 2.40 | 1.96 |

IV. SUMMARY

In conclusion, we have demonstrated for the first time that at low temperature, the methanethiol S atoms form dimers when adsorbed on the regular Au(111) surface [11]. As the temperature rises, these dimers dissociate. The S atoms in methylthiolate do not dimerize at 1.0 ML, while a dimer emerges as most stable at 0.5 ML. With increasing temperature the S-S distance of two adjacent methylthiolate molecules shortens, leading to the formation of the experimentally observed dialkyl disulfide. This chemical dimer emerges during the desorption process and does not exist on the surface. Prior to this study, it was assumed that methanethiol and methylthiolate realize the same pattern upon adsorption on the Au(111) surface. This assumption was based on the

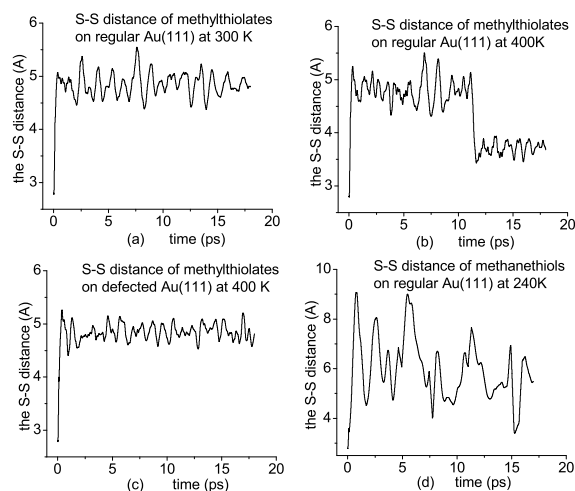


FIG. 2: Time variation of the S-S distance in four cases.

premise that methanethiol deposited on a gold substrate turns into methylthiolate. This proposition, however, has turned out to be fallacious. As demonstrated by both experiment and theory [11, 12], methanethiol persists on the clean Au(111) surface, and this work establishes that methanethiol and methylthiolate display distinctly different dimerization patterns. Our results thus resolve the long-standing controversy over the correct interpretation of the experimental data related to the dimer formation by methanethiol and methylthiolate headgroups on the Au(111) surface.

Acknowledgments

This work is supported by the NSF through Grants HRD-9805465 and DMR-0304036, by NIH through Grant S06-GM008047, by AHCRC under Cooperative Agreement No. DAAD 19-01-2-0014, and by DoD through Contract #W912HZ-06-C-005.

- [1] P. Fetner, A. Eberhardt, P. Eisenberger, *Science* 266, 1216 (1994).
- [2] P. Fenter, F. Schreitberger, L. Berman, G. Scoles, P. Eisenberger, M. Bedzyk, *Surf. Sci.* 412, 213 (1998).
- [3] G. Kluth, C. Carraro, R. Maboudian, *Phys. Rev. B* 59, R10449 (1999).
- [4] H. Gronbeck, A. Curioni, W. Andreoni, *J. Am. Chem. Soc.* 122, 3839 (2000).
- [5] M. Vargas, P. Giannozzi, A. Selloni, G. Scoles, *J. Phys. Chem. B*, 105, 9509 (2001).
- [6] L. Molina, B. Hammer, *Chem. Phys. Lett.* 360, 264 (2002).
- [7] Y. Yourdshahyan, A. Rappe, *J. Chem. Phys.* 117, 825 (2002).
- [8] H. Kondoh, M. Iwasaki, T. Shimada, K. Amemiya, T. Yokoyama, T. Ohta, *Phys. Rev. Lett.* 90, 066102 (2003).
- [9] T. Shimada, H. Kondoh, I. Nakai, M. Nagasaka, R. Yokota, K. Amemiya, T. Ohta, *Chem. Phys. Lett.* 406, 232 (2005).
- [10] P. Maksymovych, D. Sorescu, D. Dougherty, J. Yates, Jr., *J. Phys. Chem. B* 109, 22463 (2005).
- [11] I. Rzeznicka, J. Lee, P. Maksymovych, J. Yates, Jr., *J. Phys. Chem. B* 109, 15992 (2005).
- [12] J. Zhou, F. Hagelberg, *Phys. Rev. Lett.* 97, 045505 (2006).
- [13] X. Torrelles, C. Vericat, M. Vela, M. Fonticelli, M. Millone, R. Felici, T. Lee, J. Zegenhagen, G. Munoz, J. Martin-Gago, R. Salvarezza, *J. Phys. Chem. B* 110, 5586 (2006).
- [14] L. Rodriguez, J. Gayone, E. Sanchez, O. Grizzi, *J. Phys. Chem. B* 110, 7095 (2006).
- [15] F. Schreiber, *J. Phys.: Condens Matter* 16, R881 (2004); C. Vericat, M. Vela, R. Salvarezza, *Phys. Chem. Chem. Phys.*, 7, 3258 (2005).
- [16] G. Kresse, J. Hafner, *Phys. Rev. B* 47, R558 (1993); G. Kresse and J. Furthmüller, *Phys. Rev. B* 54, 11169 (1996).
- [17] G. Kresse, J. Joubert, *Phys. Rev. B* 59, 1758 (1999).
- [18] P.E. Blochl, *Phys. Rev. B* 50, 17953 (1994).
- [19] J. P. Perdew, Y. Wang, *Phys. Rev. B* 46, 6671 (1992).
- [20] H. J. Monkhorst, J. D. Pack, *Phys. Rev. B* 13, 5188 (1976).
- [21] J. Zhou, F. Hagelberg, C. Xiao, *Phys. Rev. B* 73, 155307 (2006).
- [22] A. Khein, D. Singh, C. Umrigar, *Phys. Rev. B* 51, 4105 (1995).
- [23] N. Camillone, C. Chidsey, G. Liu, G. Scoles, *J. Chem. Phys.* 98, 3503 (1993).
- [24] J. Bucher, L. Santesson, K. Kern, *Appl. Phys. A* 59, 135 (1994).
- [25] M. Preuss, W. Schmidt, F. Bechstedt, *Phys. Rev. Lett.* 94, 236102 (2005); A. Hauschild, K. Karki, B. Cowie, M. Rohlfing, F. Tautz, M. Solowski, *Phys. Rev. Lett.* 94, 036106 (2005).
- [26] Q. Chen, N. Richardson, *Nat. Mater.* 2, 324 (2003).
- [27] M. Frisch, G. Trucks, H. Schlegel, G. Scuseria, M. Robb, J. Cheeseman, J. Montgomery, Jr., T. Vreven, K. Kudin, J. Burant, J. Millam, S. Iyengar, J. Tomasi, V. Barone, B. Mennucci, M. Cossi, G. Scalmani, N. Rega, G. Petersson, H. Nakatsuji, M. Hada, M. Ehara, K. Toyota, R. Fukuda, J. Hasegawa, M. Ishida, T. Nakajima, Y. Honda, O. Kitao, H. Nakai, M. Klene, X. Li, J. Knox, H. Hratchian, J. Cross, C. Adamo, J. Jaramillo, R. Gomperts, R. Stratmann, O. Yazyev, A. Austin, R. Cammi, C. Pomelli, J. Ochterski, P. Ayala, K. Morokuma, G. Voth, P. Salvador, J. Dannenberg, V. Zakrzewski, S. Dapprich, A. Daniels, M. Strain, O. Farkas, D. Malick, A. Rabuck, K. Raghavachari, J. Foresman, J. Ortiz, Q. Cui, A. Baboul, S. Clifford, J. Cioslowski, B. Stefanov, G. Liu, A. Liashenko, P. Piskorz, I. Komaromi, R. Martin, D. Fox, T. Keith, M. Al-Laham, C. Peng, A. Nanayakkara, M. Challacombe, P. Gill, B. Johnson, W. Chen, M. Wong, C. Gonzalez, J. Pople, Gaussian 03. Gaussian, Inc.: Pittsburgh, PA, 2003.
- [28] Y. Zhao, D. Truhlar, *J. Phys. Chem. A* 110, 5121 (2006).
- [29] T. Mourik, R. Gdanitz, *J. Chem. Phys.*, 116, 9620 (2002);

- A. Milet, T. Korona, R. Moszynski, E. Kochanski, J. Chem. Phys., 111, 7727 (1999); T. Wesolowski, J. Chem. Phys., 113, 1666 (2000).
- [30] R. Mazzarello, A. Cossaro, A. Verdini, R. Rousseau, L. Casalis, M. Danisman, L. Floreano, S. Scandolo, A. Morgante, G. Scoles, Phys. Rev. Lett. 98 , 016102 (2007).